^{3}He tube counters as detectors for atmospheric neutron spectral measurements

ANATOLY GUSEV
Department of Space Geophysics, Space Research Institute of the Russian Academy of Sciences (IKI) Moscow
RUSSIA

INACIO M. MARTIN
MAURO A. ALVES
Technological Aeronautics Institute (ITA), São José dos Campos, SP
BRASIL

Abstract: Response matrices for ^{3}He proportional neutron counters of spherical and cylindrical form were simulated. It is shown that the latter can be converted to the first with simple linear operation, what points to tube counters, as a potential device for neutron spectrum observation.

Keywords*:* Bonner sphere, atmospheric neutrons, tube counter, Monte Carlo simulation

Received: June 26, 2022. Revised: January 2, 2023. Accepted: February 7, 2023. Published: March 1, 2023.

1. Introduction

Bonner Sphere Spectrometer (BSS) [1] is one of the systems most commonly employed in neutron spectrometry [2] and is a a unique device suitable for spectral observation of thee environmental neutron background [3].

BSS in its traditional configuration consist of a set of thermal neutron detectors like proportional counters of spherical form filled with ^{3}He or BF_3 embedded in a thermalizer i.e. a scattering material like polyethylene decreasing neutron energy down to thermal one (see Fig. 1),

In the case of ^{3}He-filled counter, a neutron causes the breakup of ^{3}He nucleus into a tritium nucleus ^{3}H and a proton. The triton and the proton share the reaction energy Q.

$$^3\text{He} + n(\text{thermal}) \rightarrow p + {}^3\text{H} + Q, \quad Q = 764\ keV \qquad (1)$$

An increase of a thermalizer thickness results in decrease of detection efficiency of less energetic neutrons relatively to more energetic ones, that make it possible to estimate the

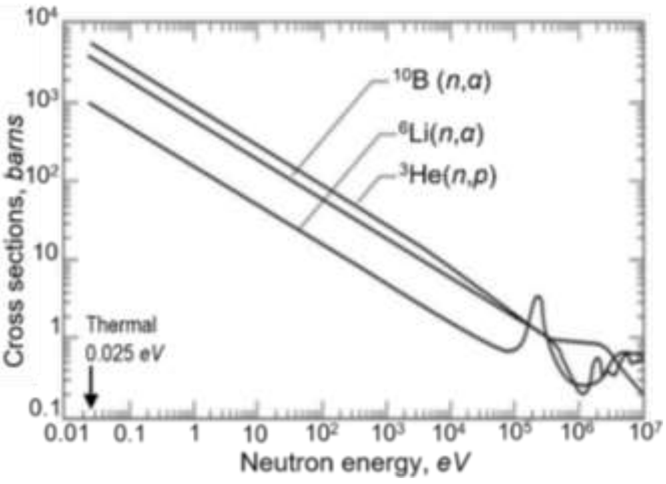

Fig.1. Neutron capture cross sections of ^{3}He, ^{10}B, ^{6}Li. [4]

spectral composition of the neutron flux.

That dependence is maximally pronounced for counters of a spherical form because it provides maximum volume with minimum dimensions and thus proved to be less sensitive to energetic neutrons with ranges exceeding the diameter of the sphere. An additional advantage of a spherical detector is its symmetry providing independence of its isotropic response to an incident flux.

An output (i.e count rate) $C_i(T_i)$ of a counter numbered i with a thermalizer of a thickness T_i is

$$C_i(T_i) = \int_{E}^{E_{max}} F(E) R_i(T_i, E) dE \qquad (2)$$

where $F(E)$ is a desired flux of neutrons with energy E. A set of functions $R_i(T_i,E)$ is a so called "response matrix" which describes registration efficiency of a counters with thermalizer thicknesses T_i.

In order to restore a measured spectrum $F(E)$ from a readings C_i of a set of N detectors one need to solve a system of N integral equations (1), which has no a unique solution for a reasonable number of detectors. Instead of that another problem is solved, namely, a search for a spectrum $F(E)$ as close as possible to some predetermined one. It is clear that the more detectors are used and statistics accumulated, the more accurate approximation will be obtained. For this reason, number of the detectors in modern experimental exceeds a dozen.

As for atmospheric neutron observation, its specific problem is quite low intensity of their flux (see fig. 2). In the same time maximal diameters of spherical counters commercially produced does not exceed 5 cm [5]. That impedes accumulation of statistics needed both for accurate determination of its spectrum and reliable detection of actual changes in it.

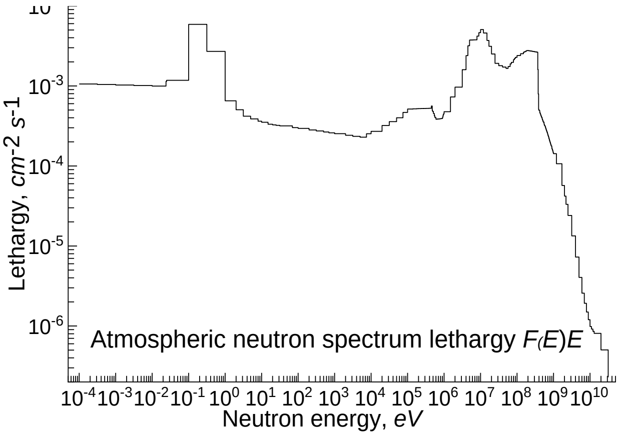

Fig. 2. A lethargy spectrum of the atmospheric neutron spectrum at the sea-level. It is a combination of a spectrum experimentally measured in Sao Jose dos Camps (Brazil, 23°10'44"S 45°53'13"W, 900 m altitude) [3] (up to 10^8 *eV*) and for energies above that from JEDEC JESD89A standard [6] for the same location.

In this work we considered a possibility of using more simple cylindrical proportional counters. That type of counters of large sizes of up to 2 *m* long, and 30 *cm* diameter are widely used in cosmic ray monitors [7,8] and soil moisture monitoring [9].

For this response matrices for spherical and cylindrical counters were simulated. The modern toolkits for simulation of the passage of particles through matter allow perform such a simulation with any needed accuracy.

2. Simulation model

The simulation was performed with Geant4 [10] – a large-scale particle physics package based on Monte-Carlo method. Data on reaction cross sections, neutron multiple scattering and particle propagation through the matter were taken from QGSP_BIC_HP Physics list [11] containing high precision neutron model for neutrons below 20 *MeV* energy. Edition and compilation of the program code was performed in Windows Visual C++ environment. Executable code was produced with CMake tool.

The geometry configuration of the simulation model is shown in Fig.3.

Contrary to tube counters the efficiency of spherical counters is isotropic. But because the neutron ground level background is known to be also isotropic [12,13] the both geometries are equivalent in this case.

The response matrices were simulated for a spherical

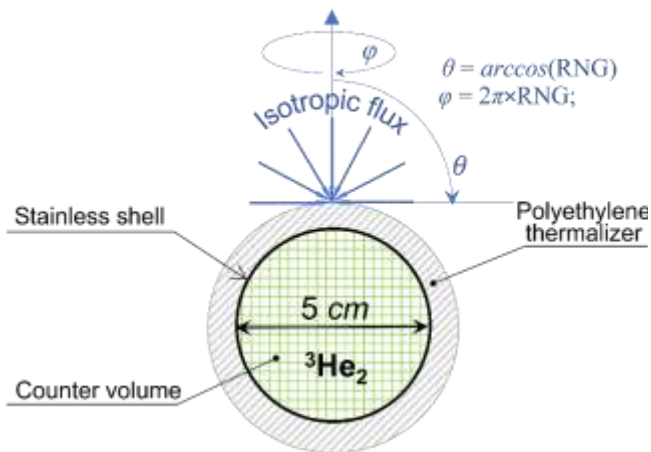

Fig. 3. A geometry considered in the simulation. RNG is a Random Number Generator from 0 up to 1

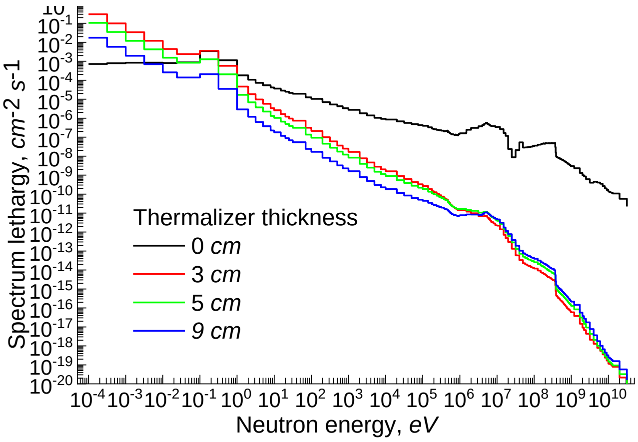

Fig.4 Integrands Eq.1 for spheric detectors

counter of 5 *cm* diameter and for a cylindrical counter of the same diameter and of 30 *cm* length (like used in the COSMOS project [9]) for bare counters and those with polyethylene thermalizer of 3, 5, and 9 *cm* thickness (like in [14]). Simulation was performed for neutron energies in the range 10^4–$3\cdot10^{11}$ *eV*. Number of samplings varies from 10^3 to $3\cdot10^9$ depending on reaction cross section (Eq.1) for corresponding neutron energy (Fig.1). Integrands in Eq.2 were calculated using the spectrum in Fig.2.

3. Results and discussion

Fig.5 in the APPENDIX presents the simulated response matrices. Example of the corresponding integrands in Fig.4 demonstrates detector response to the atmospheric spectrum in Fig.2. The curves for the tube detectors are normalized for corresponding outputs C_i (Eq.2) presented in Tab.1. Note that the output does not monotonously depend on thermalizer thickness (line 3).

It is easy to see that the curve shapes for tube and sphere counters in Fig.5 coincide when the same thermalizer thicknesses. Thus, the matrix for the tubes can be converted to that for the sphere one with a simple linear operation. Due to that, the Eq.2 has the same solution for the both geometries and are essentially equivalent in this point.

The difference between outputs of the counters (see line 5 of the Table 1) and statistical error determine an accuracy of a solution: the more difference and the larger statistics accumulated the higher accuracy of a solution. As it should be expected this first parameter is better for spherical counters. However, this difference proved to be less than two. In the same time the values of the normalization coefficients rise with thermalizer thicknesses thus reflecting more weak dependence of the tube detectors on neutron energy being compared with the spherical ones. That may result to less accurate determination of the spectrum via unfolding However, at least partially this shortage could be offset by increased statistics accumulated with lager tube counters. For example, the sensitive surface of the spherical detector

Table 1. Simulated output of tube and spheric detectors

1	Detector number ***i***		1	2	3	4
2	Thermalizer thickness		0 *cm*	3 *cm*	5 *cm*	9 *cm*
3	Detector output per cm^2 C_i	Tube	$1.2\cdot10^{-2}$	$0.32\cdot10^{-2}$	$2.7\cdot10^{-2}$	$0.09\cdot10^{-2}$
		Sphere	$2.7\cdot10^{-2}$	$0.13\cdot10^{-2}$	$0.82\cdot10^{-2}$	$0.02\cdot10^{-2}$
4	C_i tube / C_i sphere		1.26	2.43	3.30	4.57
5	Detector output ratio $C_i / C_{i\text{-}1}$	Tube		3.66	0.12	30.1
		Sphere		7.1	0.16	41.6

considered here is 25π cm^2 and that of the cylindrical is 150π cm^2.i.e. 6 times more The registration efficiency of the latter with 3 *cm* thermalizer is 2.4 higher and for 5 *cm* one is 3.3 higher. The corresponding narrowing of margins of error is $\sqrt{6 \cdot 2.4} \approx 3.8$ and $\sqrt{6 \cdot 3.3} \approx 4.4$ times being compared with those of the spherical counter that quite compensate decrease of difference in the case of tube counter.

4. Conclusion

A response of neutron detectors of spherical and cylindrical geometries to the ground level atmospheric neutron spectrum was performed using Geant4 package. Comparison of response matrices of the two geometries showed their identity up to a coefficient. This in turn should provides identical unfolded spectra.

At the same time the cylindrical geometry demonstrated weaker dependence on thermalizer thickness being compared to the spherical one. That may result to lower accuracy of an unfolding procedure. It is shown that this shortage can be compensated at list partially by increased registration efficiency and sensitive surface of cylindrical counters. Thus, result of the simulation allows tube counters to be considered as a potential device for radiation environut monitoring.

Reference

[1] D. Thomas , A. Alevra, Bonner sphere spectrometers - a critical review, Nucl. Instrum. Meth. A: vol. 476, pp. 12-20, 2002

[2] H. Mazrou , A. Nedjar , T. Seguini, Neutron spectrum measurements at a radial beam port of the NUR research reactor using a Bonner spheres spectrometer, Applied Radiation and Isotopes, vol. 114, pp. 63-70, 2016

[3] C. Federico, O. Gonçalez, E. Fonseca, I. Martin, L. Caldas, - *Neutron spectra measurements in the South Atlantic anomaly region,* Radiat. Meas., vol. 45, pp. 1526-1528, 2010

[4] S. Tavernier, Introduction, Experimental Techniques in Nuclear and Particle Physics. Springer, Berlin, Heidelberg, 2009

[5] 2705 Helium-3 Neutron Detector, https://www.lndinc.com/products/neutron-detectors/2705/

[6] Process Management for Avionics—Atmospheric Radiation Effects. Guidelines for Single Event Effects Testing for Avionics Systems; IEC Standard 62396-2; International Electrotechnical Commission: Geneva, Switzerland, 2017

[7] P. Stoker, L. Dorman, J. Clem, *Neutron Monitor Design Improvements*, Space Science Review, vol. 93, pp. 361-380, 2000

[8] T. Kuwabara, J. W. Bieber, J. Clem, et al., Real-time cosmic ray monitoring system for space weather, SPACE WEATHER, DOI:10.1029/2005SW000204, 2006,

[9] M. Zreda, W. Shuttleworth, X. Zeng, , et al., COSMOS: The cosmic-ray soil moisture observing system, Hydrol. Earth Syst. Sci., 16, 4079–4099, https://doi.org/10.5194/hess-16-4079-2012, 2012.

[10] J. Allison, K. Amako, J. Apostolakis, et al., *Recent developments in Geant4*, Nucl. Instrum. Meth. A, vol 835, pp. 186-2251, 2016

[11] J. Apostolakis, G. Folger, ;V. Grichine, et al., Progress in hadronic physics modelling in Geant4, J. Phys.: Conf. Ser. 160, pp. 012073, 2009

[12] H. Wulandari, J. Jochum, W. Rau, F. von Feilitzsch, Neutron Background Studies for the CRESST Dark Matter Experiment, arXiv:hep-ex/0401032, 2004

[13] M. Pazianotto, M. Cortés-Giraldo, C. Federico , et al., Analysis of the angular distribution of cosmic-ray-induced particles in the atmosphere based on Monte Carlo simulations including the influence of the Earth's magnetic field, Astroparticle Physics, v. 97, pp. 106-117, 2018

[14] H. Matsumoto, T. Goka, K.Koga et al., *Real-time measurement of low-energy-range neutron spectra on board the space shuttle STS-89 (S/MM-8)*, Radiat. Meas., vol. 33, pp. 321-333, 2001

Appendix

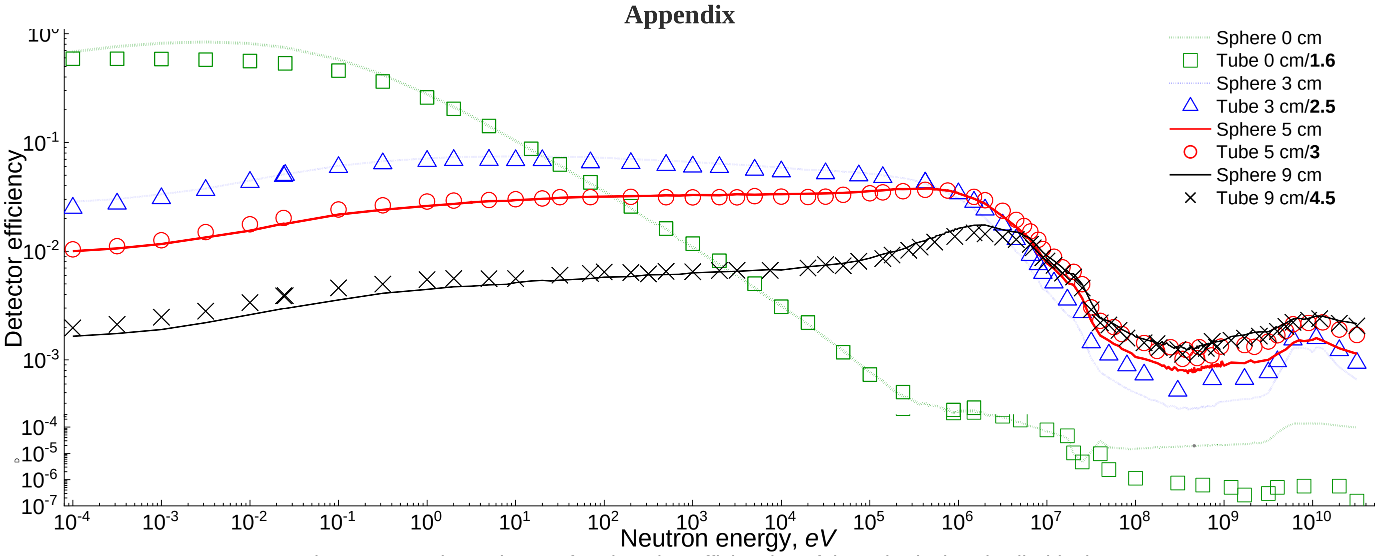

Fig.5. Energy dependence of registration efficiencies of the spherical and cylindrical counters with different thermalize thicknesses for an isotropic neutron flux